High-speed noncontact profiler based on scanning white-light interferometry

Leslie Deck and Peter de Groot

We describe a system for fast three-dimensional profilometry, of both optically smooth and optically rough surfaces, based on scanning white-light techniques. The system utilizes an efficient algorithm to extract and save only the region of interference, substantially reducing both the acquisition and the analysis times. Rough and discontinuous surfaces can be profiled without the phase-ambiguity problems associated with conventional phase-shifting techniques. The system measures steps to 100 μm, scans a 10-μm range in 5 s, and has a smooth surface repeatability of 0.5 nm.

Introduction

Optical interferometric profilers are widely used for three-dimensional profiling of surfaces when noncontact methods are required. These profilers typically use phase-shifting interferometric (PSI) techniques and are fast, accurate, and repeatable, but suffer from the requirement that the surface be smooth relative to the mean wavelength of the light source. Surface discontinuities greater than a quarter-wavelength (typically 150 nm) cannot be unambiguously resolved with a single-wavelength measurement because of the cyclic nature of the interference. Multiwavelength measurements can extend this range, but the constraints imposed on wavelength accuracy and environmental stability can be severe.[1]

Profilers based on scanning white-light interferometry (SWLI) overcome many of the limitations of conventional PSI profilers for the measurement of rough or discontinuous surfaces. A number of articles describe this technique in detail.[2–7] Typically these profilers record the position of a contrast reference feature (i.e., peak contrast or peak fit) for each point in the field of view while axially translating one arm of an equal-path interferometer illuminated with a broadband source. A common problem with this technique is the enormous amount of computation required for calculating the contrast for each point in real time. Often the contrast calculation alone is insufficiently precise because of the discrete sampling interval, forcing either an increase in the sampling density or incorporating an interpolation technique, both of which further slow the acquisition process.

In this paper we present a new approach to data acquisition for SWLI-based instruments that permits data acquisition to proceed at much higher rates than previously possible with only modest amounts of fast memory while retaining the complete interferogram for later processing. These data are then analyzed by frequency-domain analysis[8] for the final calculation of the surface heights. Possession of the complete interferogram permits many novel capabilities, such as source spectrum compensation and true color processing.

Apparatus

The SWLI profiler is illustrated in Fig. 1. Broadband light from a tungsten-halogen lamp is directed by a beam splitter to a Michelson- or Mirau-type interferometric objective. A piezoelectric transducer (PZT) translates the objective as much as 100 μm along the optical axis. The PZT is precalibrated to provide highly repeatable and accurate constant velocity motion. The scan rate is variable but is nominally set at 2.025 μm/s. The interferogram is imaged onto a video camera, and the video is digitized to 8-bit precision by a frame grabber during the PZT scan. Each frame is transferred to the host computer, which performs the acquisition and analysis functions and controls the PZT scan initiation and rate.

The authors are with the Zygo Corporation, Laurel Brook Road, Middlefield, Connecticut 06455-0448.

Received 16 July 1993; revised manuscript received 16 May 1994.

0003-6935/94/317334-05$06.00/0.

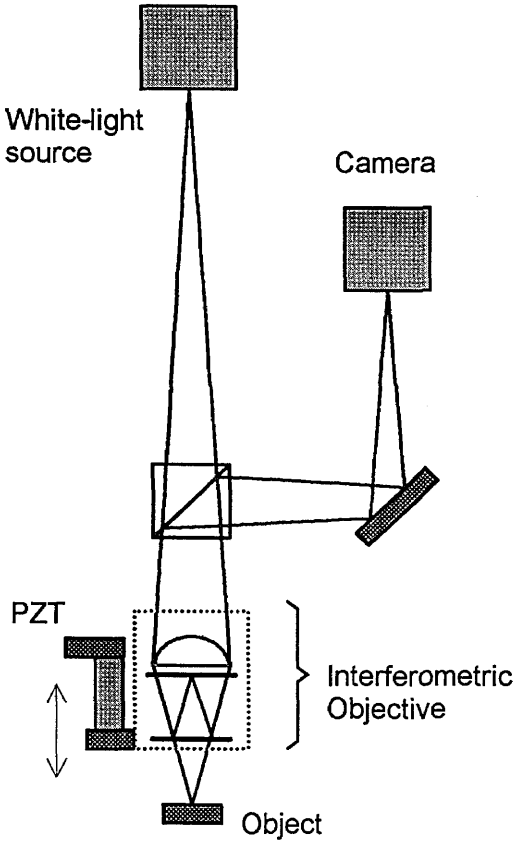

Fig. 1. Schematic diagram of the SWLI profiler. PZT, piezoelectric transducer.

Acquisition

A typical pixel-intensity time history for a relatively weak interference signal during a 100-μm scan is illustrated in Fig. 2. The interference is extremely localized, generating a sharply defined coherence region only a few micrometers wide. The rest of the distribution represents low-frequency background illumination that stems from test surface scatter and defocus. For profiling purposes, only the interference region and its location in the scan are important. Thus, for optimal speed and efficiency with a minimum of resources, the acquisition should ignore everything except the data about the interference region. There are five requirements for doing this effectively. First, the interference region must be identified. Second, the system must acquire data symmetrically placed about the interference peak for each pixel. Third, the complete interferogram must be acquired. Fourth, the position of the acquired data relative to the total scan must be saved. Fifth, this must be done quickly, with a minimum of computation.

The first requirement is fulfilled with a simple frequency-based discriminator that identifies the modulation region. As Fig. 2 makes clear, the discriminator cannot be amplitude based because of the possibility of large-amplitude backgrounds. The interference frequency has a relatively well-defined range because the PZT translation rate is precisely controlled and the mean source wavelength is known to within ~10%. If the scan provides approximately 90° of fringe shift per frame, a discriminator that consists of the difference between the intensity seen in the current frame and that seen two frames before (i.e., frames separated by 180°) has a variation proportional to the interference amplitude. Figure 3 illustrates the discriminator values calculated from the pixel-intensity history in Fig. 2. Although the specific behavior of this discriminator is dependent on the frame spacing and on the phase offset between fringe and frame, it is extremely effective in localizing the interference region over a broad range of fringe frequencies for strongly peaked coherence functions, such as those produced from broadband sources. As is made clear below, our implementation is unaffected by the fact that this discriminator does not produce continuous fringe contrast information.

The second through fourth requirements are satisfied by the use of a circular buffer for data acquisition. For each pixel, a sequence of consecutive memory locations acting as a circular buffer of predetermined size (Q) is set up. A single buffer pointer identifies

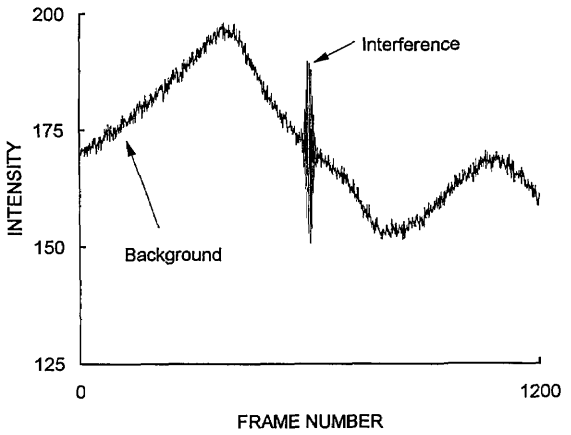

Fig. 2. Intensity history from a single pixel during a 100-μm scan when a broadband source is used. The intensity, digitized to 8-bit precision, versus the camera frame number is plotted during the scan.

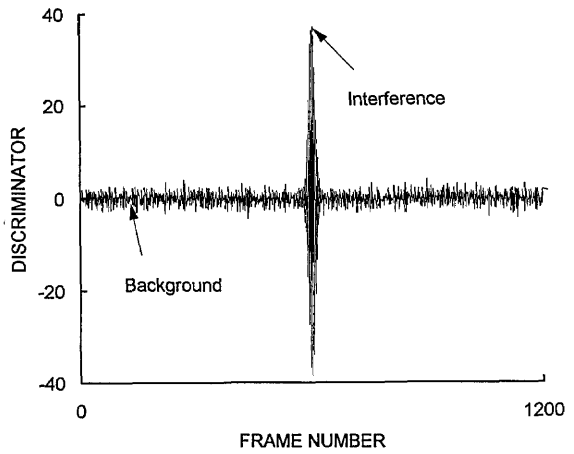

Fig. 3. Plot of the calculated discriminator for the pixel history shown in Fig. 2.

the current storage location for all the pixels and is incremented each frame. The pointer wraps around to the beginning of the buffer when the end of the buffer is reached. Additionally, each pixel is provided with two memory locations, one that saves the frame number when the maximum discriminator level is seen and the other that saves the value of the maximum. After a frame is received, the discriminator is calculated for each pixel and is compared with the last saved maximum. If larger, it replaces the older maximum, the frame number is saved, and the pixel intensity is saved in the circular buffer at the position indicated by the buffer pointer. If it is smaller than the previously saved maximum and less than $Q/2$ frames have transpired since the last saved discriminator maximum, the pixel intensity is also saved as before. Otherwise the data are discarded. This operation is illustrated in Fig. 4 for a Q of 16. At the end of the procedure each circular buffer contains a set of contiguous (i.e., taken at successively contiguous camera frames) intensity values straddling the coherence maximum. The saved peak discriminator frame number gives the relative position of the data set in the total scan, and the position of the discriminator maximum in the buffer is determined by the calculation of the peak frame number modulo Q. Thus, as long as new peak discriminator information occurs before $Q/2$ frames have transpired, the algorithm always captures at least $Q/2$ consecutive frames. Under typical conditions a new useful discriminator peak occurs every fourth sample.

The choice of buffer size depends on the coherence width or, equivalently, on the source spectrum. For our source spectrum, which is approximately Gaussian with a full-width at half-maximum of ~100 nm centered about 630 nm, and for sampling every 90° of phase, a Q of 40 (~3.2-μm total width) is adequate to

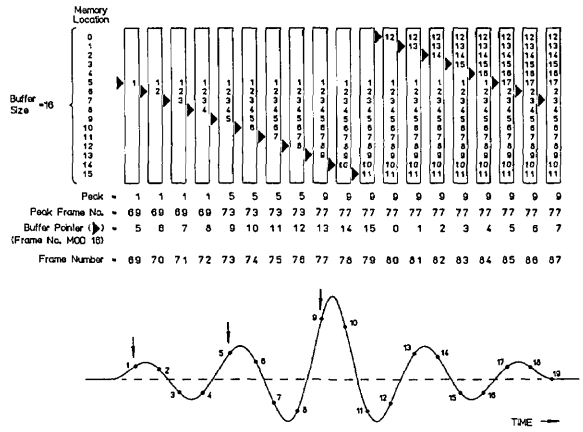

Fig. 4. Representation of the circular buffer scheme implemented in the SWLI profiler for a buffer (Q) size of 16. For one pixel, the positions of the acquired intensity data near the interference region are shown as points on the curve at the bottom. The positions of a new peak in the discriminator are indicated with arrows. Directly above each point, the circular buffer contents (vertical rectangles) as well as the frame number, discriminator peak frame number, and buffer pointer are shown at that point in the acquisition.

guarantee coverage of the envelope. Less than 3 Mbytes of solid-state memory is required for implementing this acquisition procedure for a Q of 40 and a 256^2 image size at 8-bit precision. This should be compared with the over-87 Mbytes of storage required for saving all the data from a 100-μm scan. The memory requirements of the algorithm are independent of the scan length, and all operations can be performed with integer arithmetic. Using a HP700 computer, we have achieved acquisition rates of 2 million pixels/s (30 Hz for a 256^2 frame). Significantly higher acquisition rates can be expected with dedicated hardware. Thus the fifth requirement is also satisfied.

Assuming an adequate buffer size, the algorithm can still fail under conditions for which the coherence width is either too narrow or contains significant mode structure. The contrast in an extremely narrow coherence peak rises so sharply that sufficient data before the contrast peak may not be saved. In practice this implies a source spectrum broader than the typical passband of most commercial objectives so is usually not a problem except for extremely high numerical aperture objectives, where the spatial coherence properties can also strongly affect the interference width. On the other hand, spectrally apertured sources or sources with comb spectra (typical in multimode laser diodes, for example) produce coherence functions with numerous sidelobes. If these sidelobes are encountered during the scan, they can raise the maximum discriminator level before the start of the main coherence lobe, so the algorithm discards main lobe data until the discriminator exceeds the maximum set at the highest previous sidelobe. We avoid this by structuring the source spectrum to approximate a Gaussian. A Gaussian spectrum produces a Gaussian coherence shape, eliminating sidelobes and, as a consequence, minimizing the size of the circular buffer.

Acquiring the complete interferogram in this manner has many distinct advantages over simply searching for a specific reference feature. We have mentioned the reduction in computational requirements, which leads to higher throughput. But this increased throughput translates directly into a reduction in vibration sensitivity, always a concern in interferometric measurements, and leads to higher measurement accuracy and repeatability. Other unique capabilities include the accessibility of the source spectrum by a Fourier analysis of the interferogram, which, we show, permits compensation for changes in the illumination spectrum from source- or object-induced effects and the evaluation of the object's true color.

Analysis

Surface profiling in SWLI is commonly performed by the calculation of the fringe contrast envelope point for point by the use of, for example, digital demodulation techniques[9,10] and by the determination of the position of maximum contrast by the fit of the

contrast data near the peak. The efficacy of this technique depends on how well the phase separation between adjacent frames corresponds to that expected by the demodulation algorithm. As the effective mean wavelength seen by the imaging sensor will depend on the source spectrum and the dispersion and reflectivity characteristics of the object, a particular phase separation cannot be guaranteed. Furthermore, dispersion can distort the envelope, which makes the accuracy dependent on the choice of contrast reference feature. Therefore we analyze the data in the frequency domain.[8] This entails Fourier transforming the data and measuring the phase slope of the Fourier components. As the group-velocity optical path difference is given by $z = d\phi/d\omega$, the phase slope $d\phi/d\omega$ is a measure of the distance from the start of the acquired data set to the zero optical path difference position.[11] This analysis is independent of the sampling period and source characteristics as long as sufficient data are taken to ensure a complete sampling of the interferogram.[12] The phase slope, along with the saved peak frame number, frame rate, and scan velocity, is then used to calculate a surface height at each pixel location. The result is a topographical map of the surface.

For optically smooth and homogeneous surfaces, the measurement repeatability can be further improved by the use of the overall phase-offset information.[8] The analysis can then improve the resolution of smooth, homogeneous surfaces to subnanometer precision without the necessity of an additional PSI measurement. Of course, if the surface is not optically smooth or is inhomogeneous, the assumption that the measured phase is a good representation of the surface topography may not hold, and errors that are due to speckle or phase change on reflection effects can distort the profile, just as in PSI measurements.

The analysis just described is performed completely on the host processor, with the fast Fourier-transform computation taking the bulk of the processing time. With a HP700 platform and 64-point integer fast Fourier transforms, it takes typically 11 s to process a 256^2 pixel field.

Results and Conclusions

Figure 5 shows the profile from a measurement of a 20.37-μm step-height standard made with a SWLI profiler. The acquisition took only 11 s. The mean step height measured was 20.25 ± 0.02 μm, which is in good agreement with the quoted step. A step height of 20.27 ± 0.02 μm was obtained with a remeasurement with a 2.0-optical-density neutral density filter installed after the source and with the source current increased to compensate for the reduction in intensity. The mean wavelength decreased by 3.8% from 583 to 561 nm, but the measured step height was unchanged to within 0.10%, which shows the utility of having a running source mean wavelength calculation. Figure 6 is a profile of a 921-nm-high grating and is a good example of a surface that

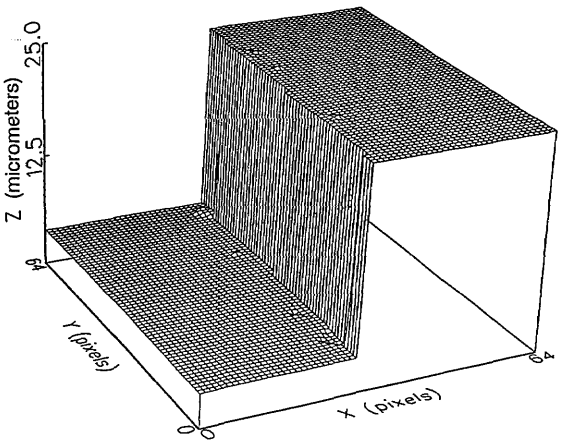

Fig. 5. Measurement of a 20.37-μm step-height standard measured with the SWLI profiler.

cannot be measured with single-wavelength PSI techniques. The average grating height was measured to be 915 nm. The data were acquired in 5 s. To test the measurement repeatability, we found that the difference between two successive measurements of a smooth flat achieved a residual of 0.43 nm rms, independent of scan length. For time-critical applications the scan rate can be increased to take fewer frames per fringe with only a small loss in repeatability. This was demonstrated with another scan of 3 frames per fringe on the 20-μm step standard. The acquisition time was reduced from 11 to 8 s but the flat repeatability degraded to 0.9 nm rms. The measured step height remained the same.

In conclusion, we have developed a high-speed interferogram acquisition algorithm for SWLI profilers. Both acquisition and analysis times are substantially reduced over conventional SWLI methods and compare favorably with PSI techniques. The data acquired are ideally suited for analysis by the use of Fourier-transform methods, and the resulting profiles enjoy subnanometer resolution.

It is a pleasure to acknowledge the contributions of Carl Zanoni, Jim Biegen, Karta Khalsa, and Frank Demarest to this work.

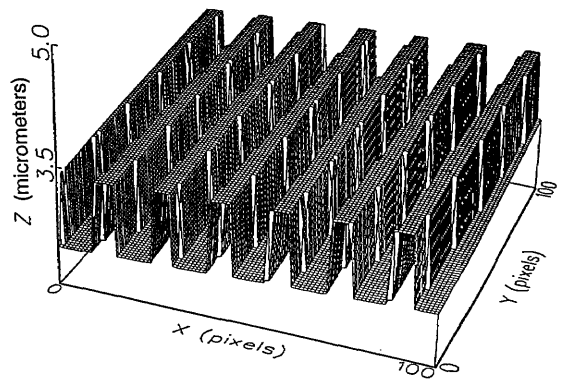

Fig. 6. Measurement of a 921-nm-high grating with the SWLI profiler.

References

1. P. J. de Groot and S. Kishner, "Synthetic wavelength stabilization for two-color laser-diode-interferometry," Appl. Opt. **30,** 4026–4033 (1991).
2. N. Balasubramanian, "Optical system for surface topography measurement," U.S. patent 4,340,306 (20 July 1982; filed 4 February 1980).
3. B. S. Lee and T. C. Strand, "Profilometry with a coherence scanning microscope," Appl. Opt. **29,** 3784–3788 (1990).
4. M. Davidson, K. Kaufman, I. Mazor, and F. Cohen, "An application of interference microscopy to integrated circuit inspection and metrology," in *Integrated Circuit Microscopy: Inspection, and Process Control,* K. M. Monahan, ed., Proc. Soc. Photo-Opt. Instrum. Eng. **775,** 233–247 (1987).
5. T. Dresel, G. Haeusler, and H. Venzke, "Three-dimensional sensing of rough surfaces by coherence radar," Appl. Opt. **31,** 919–925 (1992).
6. G. S. Kino and S. C. Chim, "Mirau correlation microscope," Appl. Opt. **29,** 3775–3783 (1990).
7. P. C. Montgomery and J. P. Fillard, "Peak fringe scanning microscopy (PFSM): submicron 3D measurement of semiconductor components," in *Interferometry: Techniques and Analysis,* G. M. Brown, O. Y. Kwon, M. Kujawinska, and G. T. Reid, eds., Proc. Soc. Photo-Opt. Instrum. Eng. **1755,** 12–23 (1992).
8. P. de Groot and L. Deck, "Surface profilometry by frequency-domain analysis of white light interferograms," in *Proceedings of the European Symposium on Optics for Productivity in Manufacturing* (EUROPTO, Frankfurt, 1994), paper 2248-13.
9. P. J. Caber, "Interferometric profiler for rough surfaces," Appl. Opt. **32,** 3438–3441 (1993).
10. S. Chen, A. W. Palmer, K. T. V. Gratten, and B. T. Meggit, "Digital signal-processing techniques for electronically scanned optical-fiber white-light interferometry," Appl. Opt. **31,** 6003–6010 (1992).
11. P. de Groot and L. Deck, "Three-dimensional imaging by sub-Nyquist sampling of white light interferograms," Opt. Lett. **18,** 1462–1464 (1993).
12. B. L. Danielson and C. Y. Boisrobert, "Absolute optical ranging using low coherence interferometry," Appl. Opt. **30,** 2975–2979 (1991).